



LAWRENCE
LIVERMORE
NATIONAL
LABORATORY

Thermal Fracture in DKDP crystals

T. Suratwala, C. Thorsness, R. Steele

September 30, 2014

Disclaimer

This document was prepared as an account of work sponsored by an agency of the United States government. Neither the United States government nor Lawrence Livermore National Security, LLC, nor any of their employees makes any warranty, expressed or implied, or assumes any legal liability or responsibility for the accuracy, completeness, or usefulness of any information, apparatus, product, or process disclosed, or represents that its use would not infringe privately owned rights. Reference herein to any specific commercial product, process, or service by trade name, trademark, manufacturer, or otherwise does not necessarily constitute or imply its endorsement, recommendation, or favoring by the United States government or Lawrence Livermore National Security, LLC. The views and opinions of authors expressed herein do not necessarily state or reflect those of the United States government or Lawrence Livermore National Security, LLC, and shall not be used for advertising or product endorsement purposes.

This work performed under the auspices of the U.S. Department of Energy by Lawrence Livermore National Laboratory under Contract DE-AC52-07NA27344.

NIF0082445/adf

MEMORANDUM – May 28, 2002

TO: File

FROM: Tayyab Suratwala, Chuck Thorsness, and Rusty Steele

SUBJECT: Thermal Fracture in DKDP crystals

One of the technical challenges of growing and fabricating KDP/DKDP crystals is to prevent its fracture. Rapid growth DKDP crystal boules grown at ‘high’ temperatures have been historically prone to fracture at the end of these ‘high’ temperature growth runs, a full-grown crystal in solution (~50°C) must be brought down to room temperature without fracture. Our goal in the following memo is to demonstrate a better understanding of thermal fracture in DKDP and propose a mitigation strategy to prevent fracture

This memo is separated into five parts. First we describe the criteria for fracture in a brittle solid and how temperature differences in the solid can cause thermal stresses (Section I). Then in section II & III one dimensional (1D) and 3 dimensional (3D) heat transfer calculations are described in order to calculate the temperature profile in DKDP exposed to different circumstances. Next the results from small size thermal shock experiments are compared with calculated temperature differences in the crystal (Section IV). Finally, in Section V an explanation is provided to why previous crystal boules fractured and then a mitigation strategy for growing DKDP rapid crystal that end at ‘high’ temperature (>45°C) is proposed.

The results of the fracture experiments and heat transfer calculations suggest that maintaining a temperature difference (ΔT) (average temperature inside the crystal – surface temperature at 20 surface edge) in air of 1 °C or less is needed to prevent fracture. Then using this criterion and comparing to the previous DKDP boule fractures observed, we conclude that the cooling of the crystal due to evaporation of solution from the crystal surface is the major contribution to the stress development. Hence we propose that during

the salt solution removal at the end of the crystal growth run (at $\sim 50^\circ\text{C}$), saturated air be input in the growth in order to prevent evaporation from the crystal surface, and then the crystal be cooled at $3^\circ\text{C}/\text{day}$.

I. CRITERIA FOR FRACTURE

The stress required for failure of a brittle material is determined by the materials toughness and the flaws present in or on the surface of the material. This concept was first illustrated by Griffith, which through a thermodynamic energy balance showed that the critical tensile stress to failure (σ_c) is given by:

$$\sigma_c = Y \frac{K_{Ic}}{\sqrt{\pi a}} \quad (1)$$

Where K_{Ic} is the fracture toughness of the material ($\text{MPa}\cdot\text{m}^{1/2}$), a is the radius of a half penny shaped flaw (m), and Y is geometric constant [1]. Figure 1 illustrates how the critical stress varies with flaw size for DKDP (average $K_{Ic}=0.10 \text{ MPa}\cdot\text{m}^{1/2}$). Notice that a DKDP crystal with a $1 \mu\text{m}$ flaw size requires $\sim 57 \text{ MPa}$ stress for failure and with a $10 \mu\text{m}$ flaw requires on only a 17 MPa stress for failure.

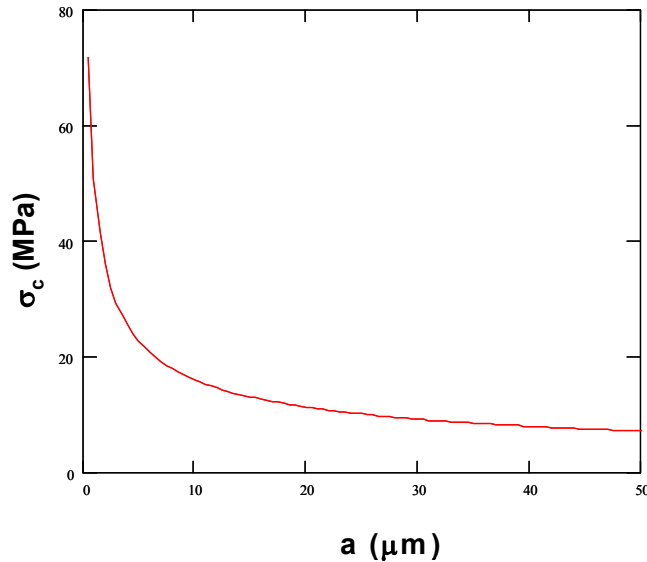


Figure 1: Calculated critical stress for catastrophic failure of DKDP as function of flaw size using Eq. (1).

Stress in the material can be caused: (1) by chemical composition changes in the material for example (see ref [2] for DKDP); (2) by external mechanical means; (3) by

changes in temperature within the material. For the case of thermal stress, difference in temperature within the material lead to one point in the material wanting to expand or shrink with respect to another point in the material. One standard approach to compare the thermal shock resistance of different materials is provided below:

$$R = \frac{(1-\nu)}{E\alpha} \frac{K_{Ic}}{\sqrt{\pi a}} \quad (2)$$

where R is the thermal shock resistance Figure-of-Merit, ν is Poisson's ratio for the material, E is the elastic modulus (GPa), α is the thermal expansion coefficient (K^{-1}). DKDP is particularly prone to thermal shock because of its low fracture toughness and high thermal expansion coefficient. Table 1 compares the thermal shock FOM for various materials.

Table 1: Comparison of the Thermal shock Figure of Merit (R) for various materials.

	DKDP/KDP	Laser Glass	Pyrex glass	Fused Silica
Fracture Toughness K_{Ic} (MPa*m^{1/2})	0.10	0.50	0.70	0.75
Thermal Expansion α (x10⁷ K⁻¹)	440	130	33	5
Elastic Modulus E (GPa)	63	47	64	70
Thermal Shock FOM for a 100 mm Flaw R (K)	1.8	34	150	1000

If we assume that DKDP is a perfectly elastic material and the major source of stress is caused thermally, than stress will only occur while there is a temperature difference in the material. Figure 2 illustrates this concept. Consider an infinite DKDP crystal slab originally at T_{init} within the crystal; no stress is present in the crystal. As the crystal is cooled, the crystal surface is at a lower temperature than its interior of the crystal. The temperature profile in the crystal is determined by the cooling rate and heat transfer properties of the crystal and environment, the calculations of the temperature profiles are discussed in more detail in section II & III. The stress profile will approximately mimic the temperature profile, and the interior of the crystal will be in compression and the outer part of the crystal will be in tension. Note that the total stress summed over the whole crystal must equal zero at all times. Hence, the point of zero stress can be

determined (see discussion below). When the whole crystal reaches the final temperature (T_{surf}); the stress at any point in the crystal again becomes zero.

Note that during cooling the surface stress is in tension and during heating the surface stress is in compression. Most flaws are present at the surface of the crystal and hence, the crystal is particularly prone to fracture during cooling.

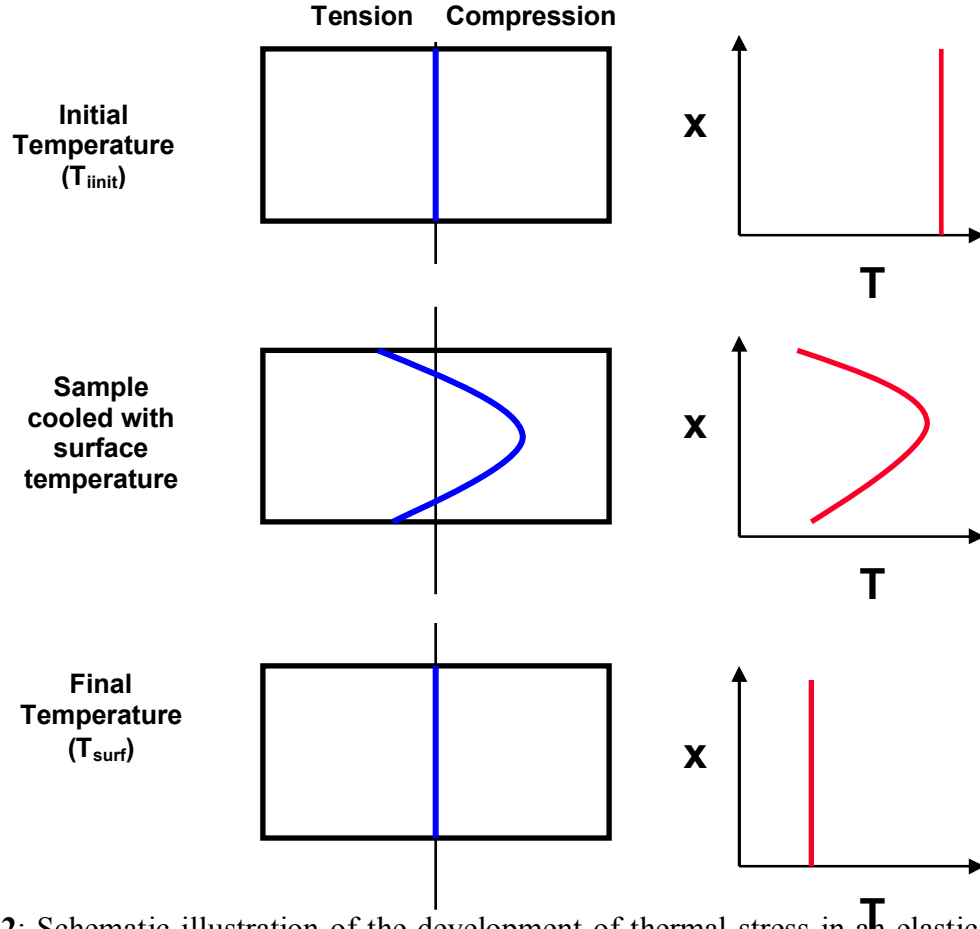


Figure 2: Schematic illustration of the development of thermal stress in an elastic solid upon cooling the solid originally at T_{init} and cooled to T_{surf} .

The stress/strain in the crystal due a particular temperature distribution in the crystal can be calculated using the elastic theory of solids[3]. This calculation for a 3 dimensional solid is a more rigorous calculation and is not examined in the current memo. However, one can estimate the maximum tensile stress for an infinite slab or a thin plate as[4]:

$$\sigma = \frac{\alpha E}{1 - \nu} (T_{ave} - T_{surf}) , \text{ for an infinite slab} \quad (3)$$

$$\sigma_t = \alpha E (T_{ave} - T_{surf}) \quad , \text{ for a thin plate} \quad (4)$$

where T_{ave} is the average temperature within the solid. The point in the solid that has the value of the average temperature is approximately the point of zero stress in the material. The value of T_{ave} in a particular crystal will depend on the heat transfer properties of the solid and the environment as well as the geometry/size of the solid. Note that the peak tensile stress is directly proportional to $T_{ave} - T_{surf}$, which we will refer to as ΔT .

The effect of size of the solid on thermal stress has been a source of confusion in recent discussions within members of LMOT including myself, to illustrate the effect of size on the stress, consider two infinite solids, one thick and one thin, initially at temperature (T_{init}) (Fig. 3). As these two solids are cooled at the same rate, temperature profile will take the shape similar to that drawn in the Figure. Notice that the T_{ave} is much lower in the thin material compared to the thick solid. Hence $T_{ave} - T_{surf}$ is much larger in the thick solid. According to Eqs. 3-4, the surface tensile stress will be larger, even though the total temperature difference in the thick solid vs thin solid is similar.

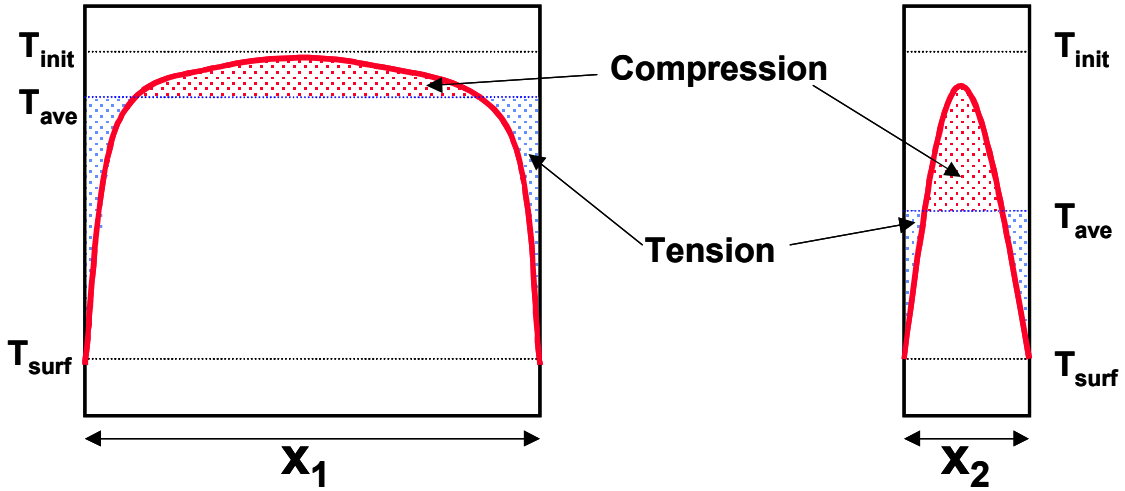


Figure 3: Comparison of the cooling of a thick solid vs a thin solid both originally at T_{init} . The tensile stress that develops at the crystal surface is proportional to the difference T_{ave} and T_{surf} (ΔT). ΔT is larger for the thicker solid compared to the thinner solid.

II. 1D HEAT TRANSFER ANALYSIS

ΔT at various times during cooling of a solid can be calculated using heat transfer analysis. In this section a simple 1D temperature analysis is used to calculate the temp profile in the crystal. In the next section a more rigorous 3D temperature analysis is described. The 1D analysis is simpler and has an analytical solution that can be solved relatively easily. The 3D analysis is more rigorous, but allows for consideration of edges and corners of the material where heat transfer could be much different leading to a much different ΔT .

For an isotropic homogeneous media the temperature as function of position x and time (t) due to conduction in the solid is given by Fourier's equation in 1D as:

$$\rho C_p \frac{\partial T(x, t)}{\partial t} = k \left(\frac{\partial^2 T(x, t)}{\partial x^2} \right) \quad (5)$$

where T is the temperature (K), k is the thermal conductivity (W/m K), ρ is the solid's density (gm/cm³), and C is the specific heat capacity of the solid (J/gm K). When convection of the environment is a contributor, Fourier's Eq above has the following surface boundary condition:

$$-k \frac{\partial T(x_b, t)}{\partial x} = h (T(x_b, t) - T_{surf}) \quad (6)$$

where x_b is the surface of solid and h is the heat transfer coefficient (W/m²K) of that boundary. Typical effective heat transfer coefficients of a solid exposed to different environments are shown in Table 2. For this analysis radiation is ignored; however the effective heat transfer coefficient can be used to approximate the contributions of convection and radiation.

Table 2: Approximate heat transfer coefficients of a solid exposed to different environment

Environment	h (W/m ² K)
1) Air only (no flow)	10
2) Water evaporation	60
3) Air only (forced flow)	100
4) Mineral Oil	200
5) Metal contact	20,000

Consider a infinite plate with thickness (2L) having a convection boundary (Fig. 4). The solution to Eq. 5 with an Eq. 6 boundary condition is then given by [5]:

$$\frac{T(x,t) - T_{surf}}{T_{init} - T_{surf}} = 2 \sum_{n=1}^{\infty} \frac{\sin(\lambda_n) \cos\left(\lambda_n \frac{x}{L}\right) \exp(-\lambda_n^2 F_o(t))}{\lambda_n + \sin(\lambda_n) \cos(\lambda_n)} \quad (7)$$

where:

$$\cot(\lambda_n) = \frac{\lambda_n}{B_i} \quad (8)$$

and B_i and $F_o(t)$ are the Biot and Fourier Modulus, respectively, which are given by [5]:

$$B_i = \frac{hL}{k} \quad (9)$$

$$F_o(t) = \frac{\alpha_T t}{L^2} \quad (10)$$

where α_T is the thermal diffusivity of the solid (cm²/sec). The relevant temperature difference in Eq. 3-4 as a function of time, is then:

$$\Delta T(t) = T_{ave}(t) - T_{surf}(t) = \frac{\int_0^L T(x,t) dx}{L} - T_{surf}(t) \quad (11)$$

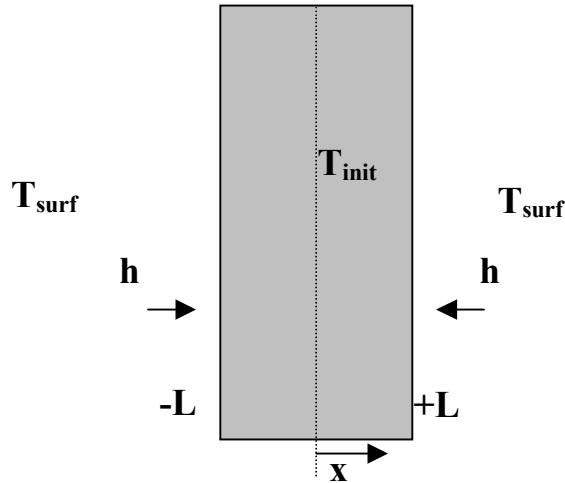


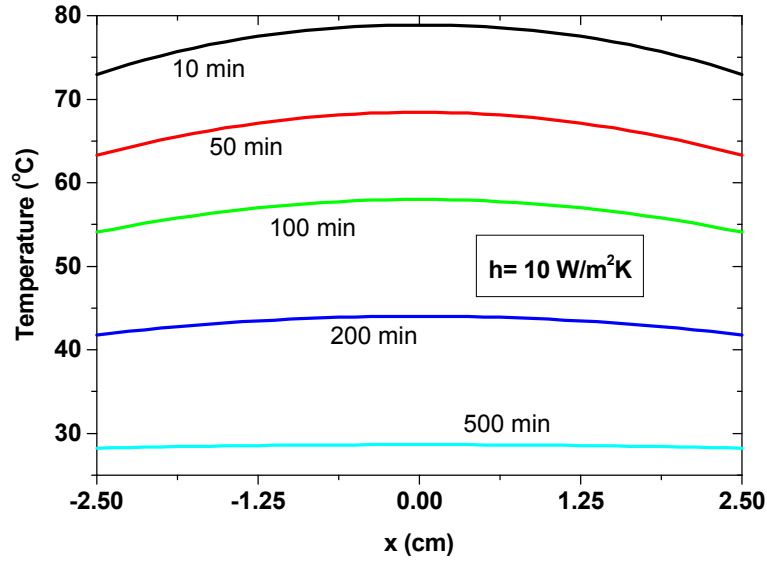
Figure 4: Coordinate system for a infinite plate of thickness (2L) with heat loss by conduction and convection.

Using the properties listed in Table 3 for DKDP, calculated temperature profiles for an infinite DKDP crystal initially at 80°C (T_{init}) and exposed to air or oil environment

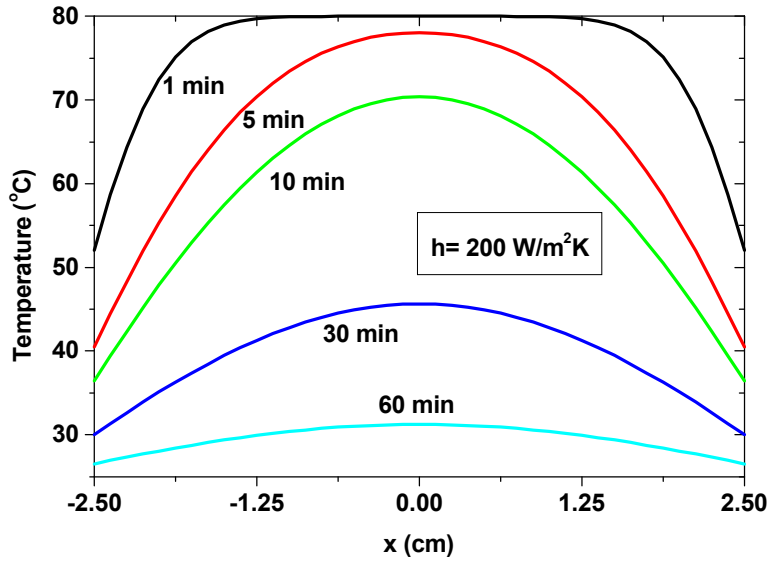
at 25°C (T_{surf}), using Eq. 7 is shown in Fig. 5. Because the heat transfer coefficient of air is much lower than that of oil, we see that there is a much smaller temperature difference at any instance in the crystal exposed to air (Fig 5a) compared to that exposed to oil (Fig 5 b). ΔT or $T_{\text{ave}} - T_{\text{surf}}$ is then plotted as function of time for these two scenarios in Fig. 6 using Eq. 11; the maximum $\Delta T = 4.1$ K occurs at 12 minutes when exposed to air, and the maximum $\Delta T = 27$ K occurs at 3 minutes when exposed to oil. It is then straightforward to calculate the maximum tensile stress using Eq. 3; $\sigma_t = 13$ MPa for air and $\sigma_t = 85$ MPa for oil. Correspondingly, under these condition the crystal exposed to air would need a flaw (2a) 38 μm to fracture and exposed to oil would need a flaw (2a) 0.9 μm to fracture. Because of the relatively small flaw sizes in both cases, it is likely that both of these crystals would fracture (see Section IV).

Table 3: Material properties of DKDP used in heat transfer analysis[6].

Property	Value for DKDP
Thermal Conductivity (k)	1.9 W/m K
Heat Capacity (Cp)	0.86 Joule/gm K
Density (ρ)	2.332 gm/cm ³
Thermal Diffusivity (α_T)	9.48x10 ⁻³ cm ² /sec
Thermal Expansion Coefficient (α)	4.4x10 ⁻⁵ K ⁻¹
Fracture Toughness (K_{Ic})	0.10 MPa m ^{1/2}
Elastic Modulus (E)	63 GPa
Poisson's Ratio (ν)	0.13



(a)



(b)

Figure 5: Calculated 1D temperature profile (from Eq. 7) at various times in a DKDP crystal of thickness 5 cm originally at 80°C and exposed to (a) air at 25°C or (b) mineral oil at 25°C.

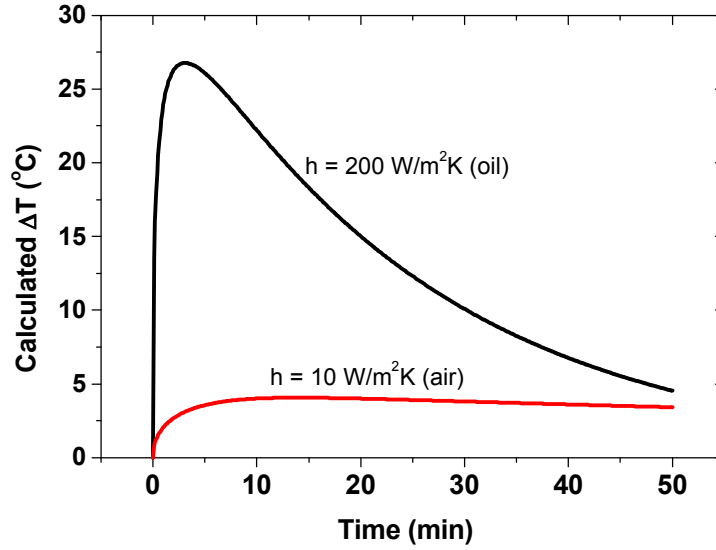


Figure 6: Calculated $\Delta T = T_{ave} - T_{surf}$ as function of time for a 5 cm thick DKDP crystal originally at 80°C and then instantly exposed to 25°C air ($h=10 \text{ W/m}^2\text{K}$) or oil ($h=200 \text{ W/m}^2\text{K}$).

III. 3D HEAT TRANSFER ANALYSIS

The 3D heat transfer analysis was performed in a similar manner as the 1D analysis. In this case, Fourier's Eq in 3D becomes:

$$\rho C \frac{\partial T(x, y, z, t)}{\partial t} = k \left(\frac{\partial^2 T(x, y, z, t)}{\partial x^2} + \frac{\partial^2 T(x, y, z, t)}{\partial y^2} + \frac{\partial^2 T(x, y, z, t)}{\partial z^2} \right) \quad (12)$$

where x , y , and z are the Cartesian coordinates. In the 3D analysis, both convection and radiation were considered; the boundary conditions then become:

$$-k \frac{\partial T(x_b, y, z, t)}{\partial x} = h (T(x_b, y, z, t) - T_{surf}) + \sigma \varepsilon (T(x_b, y, z, t)^4 - T_{surf}^4) \quad (13a)$$

$$-k \frac{\partial T(x, y_b, z, t)}{\partial y} = h (T(x, y_b, z, t) - T_{surf}) + \sigma \varepsilon (T(x, y_b, z, t)^4 - T_{surf}^4) \quad (13b)$$

$$-k \frac{\partial T(x, y, z_b, t)}{\partial z} = h (T(x, y, z_b, t) - T_{surf}) + \sigma \varepsilon (T(x, y, z_b, t)^4 - T_{surf}^4) \quad (13c)$$

where x_b , y_b , and z_b are the surfaces of the solid and σ is the Stefan-Boltzmann's constant ($\text{W/m}^2\text{K}^4$), and ε is the material's emissivity. The solutions to these set of equation's were solved using a computer based differential equation solver. Also, an analytical solution to

Equation 12 is available in reference [5]. For the 3D calculations, $h = 4 \text{ W/m}^2\text{K}$ and $\varepsilon = 0.9$ were used for DKDP.

IV. SMALL SIZE THERMAL SHOCK TESTS

A. Thermal Shock Fracture experiments

Performing thermal shock experiments can be tricky, since the failure of the part depends strongly on the flaw size in the sample. Experimentally it is quite difficult to fabricate samples with a single controlled flaw size. Instead, we have chosen the approach where the samples have been treated all the same and are assumed to have approximately the same size flaw distribution.

DKDP crystals were cut from a boule in two different geometries ($4 \times 2 \times 0.6 \text{ cm}^3$ and $2.5 \times 2.5 \times 5 \text{ cm}^3$). These crystals were cut with a band saw and no further surface finish was performed on the crystal. The samples were cut with no attempt to control the crystal orientation. Each sample was examined to see if they contained flaws greater than $500 \text{ }\mu\text{m}$ on the surface; if so, they were discarded from the experiment.

Samples were heated in an oven in air to an initial temperature (T_{init}), then the samples were removed from the oven using metal tongs covered with fiber insulation. The samples were then immediately placed either on a top of fiber insulation ($\sim 1''$ thick) or submersed in silicone oil (PDMS 200 CP) at a temperature (T_{surf}). Figure 7 illustrates schematically illustrates this procedure.

At least, five samples are used for each thermal shock condition in order gain some statistics on the failure rate.

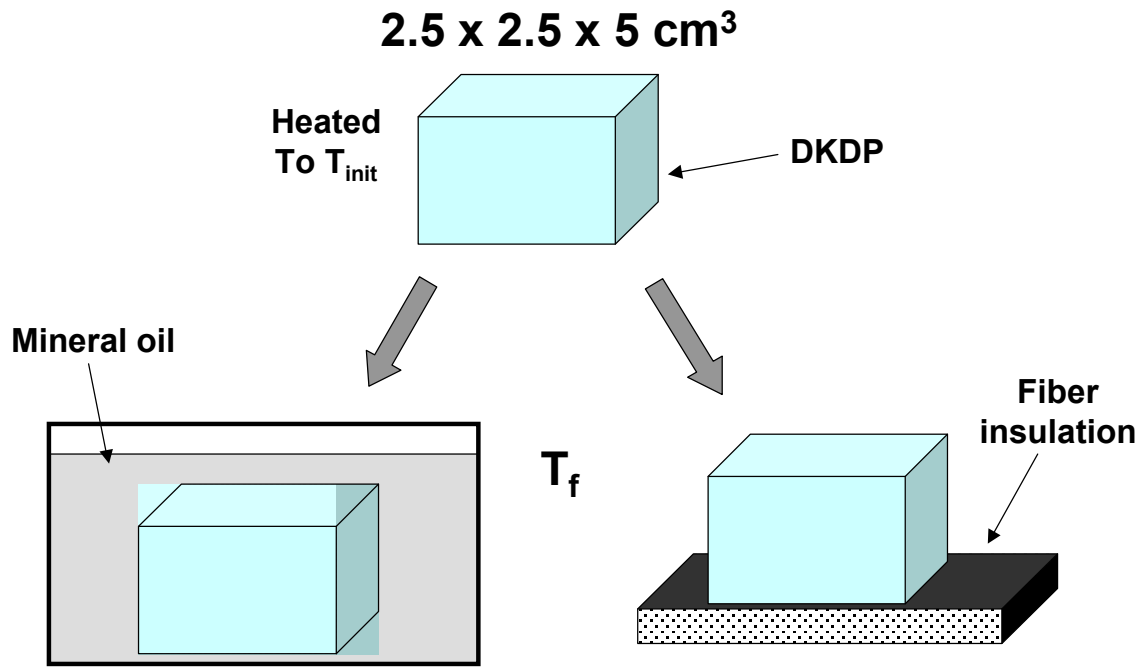


Figure 7: Schematic illustration of thermal shock experiment in mineral oil and in air.

The fracture results are summarized in Table 4 for samples quenched in air in samples. Heating the crystals to at least 60°C was required in order to observe fractures. Note that not all the samples fractured: this likely indicates differences in flaw size distributions between the samples. Samples that fractured upon air exposure initiated from the top surface at the center edge and propagated perpendicular to the vertical face of the crystal. The amount of fracture area generated increased dramatically as the exposed ΔT increase so does the stored energy. For example, the one out of five samples that fractured that were originally at T_{init} of 60°C had only a fracture that penetrated 0.5 cm into the crystal. On the other hand, samples originally at 80°C had multiple full thickness fractures.

The fracture results are summarized in Table 5 for samples quenched in oil. The results from these experiments were more consistent; either all the samples fractured or did not fracture. A temperature of 48.8°C was needed in order to cause failure. Samples that fractured various places at the edges of the crystal; typically the fractures did not penetrate very deep into the crystal.

Table 4: Results from thermal shock experiments of $2.5 \times 2.5 \times 5.0 \text{ cm}^3$ DKDP samples quenched in air on fiber insulation surface. The calculated $\Delta T = T_{\text{ave}} - T_{\text{surf}}$ and time for maximum ΔT were calculated for both the 1D and 3D heat transfer analysis. A heat transfer coefficient of $h = 10 \text{ W/m}^2 \text{ K}$ was used.

T_{initial} (°C)	T_{final} (°C)	Exposed ΔT (°C)	Observation	Fraction fractured	Measured time to fracture	1D Analysis		3D Analysis	
						Calculated $\Delta T = T_{\text{ave}} - T_{\text{surf}}$ (ΔT , °C)	Time at max ΔT (t_{max} , min)	Calculated $\Delta T = T_{\text{ave}} - T_{\text{surf}}$ (ΔT , °C)	Time at max ΔT (t_{max} , min)
87	22	65	Fractured (5/6 samples)	83%	1 min ; 10 min	2.6	2.6	2.4	3.3
77	22	55	Fractured (3/5 samples)	60%	3-6 min	2.2	2.7	2	3.5
60	22	38	Slightly Fractured (1/5 samples)	20%	3-6 min	1.5	2.7	1.3	3.7
50	22	28	No Fracture (5 samples)	0	na	1.1	2.8	0.9	4

Table 5: Results from thermal shock experiments of $2.5 \times 5.0 \times 5.0 \text{ cm}^3$ DKDP samples quenched in silicone oil. The calculated $\Delta T = T_{\text{ave}} - T_{\text{surf}}$ and time for maximum ΔT were calculated for both the 1D and 3D heat transfer analysis. A heat transfer coefficient of $h = 200 \text{ W/m}^2 \text{ K}$ was used.

T_{initial} (°C)	T_{final} (°C)	Exposed ΔT (°C)	Observation	Fraction fractured	Measured time to fracture	1D Analysis		3D Analysis	
						Calculated $\Delta T = T_{\text{ave}} - T_{\text{surf}}$ (ΔT , °C)	Time at max ΔT (t_{max} , min)	Calculated $\Delta T = T_{\text{ave}} - T_{\text{surf}}$ (ΔT , °C)	Time at max ΔT (t_{max} , min)
52.8	25.2	27.6	Fractured (4/4 samples)	100%	instantaneous	6.9	0.46	9.2	0.24
48.8	25.9	22.9	Fractured (4/4 samples)	100%	instantaneous	5.7	0.46	7.6	0.24
42.6	24.2	18.4	No Fracture (0/4 samples)	0%	na	4.6	0.46	6.1	0.24
34.6	24.4	10.2	No Fracture (0/4 samples)	0%	na	2.5	0.46	3.4	0.24

Using the 1D and 3D heat transfer analysis described in earlier sections, the maximum $\Delta T = T_{\text{ave}} - T_{\text{surf}}$ and the time at which the maximum ΔT would be observed were calculated for each of thermal shock scenarios. These values are summarized in Table 4 and 5 and also plotted against the experimental fracture results in Fig. 8. Note T_{surf} values from the 3D heat transfer analysis represents the temperatures at the surface edge of the crystal (not the surface corner) since fractures were observed to propagate only from the edge.

The results are a bit surprising; the ΔT required to observe failure in air is 1°C and 6°C for oil. If Eq. 3&4 is valid and the flaw size distribution on the crystals are essentially the same, then ΔT for failure should be same for air and oil since the stress for failure should be the same. We attribute the discrepancy to two reasons. First Eq. 2 is for an infinite slab and we are measuring fracture in block of DKDP, therefore Eq. 3 is not valid in this case. The true stress distribution in the crystal can be calculated knowing the temperature distribution in the crystal using a more rigorous computation using the elastic

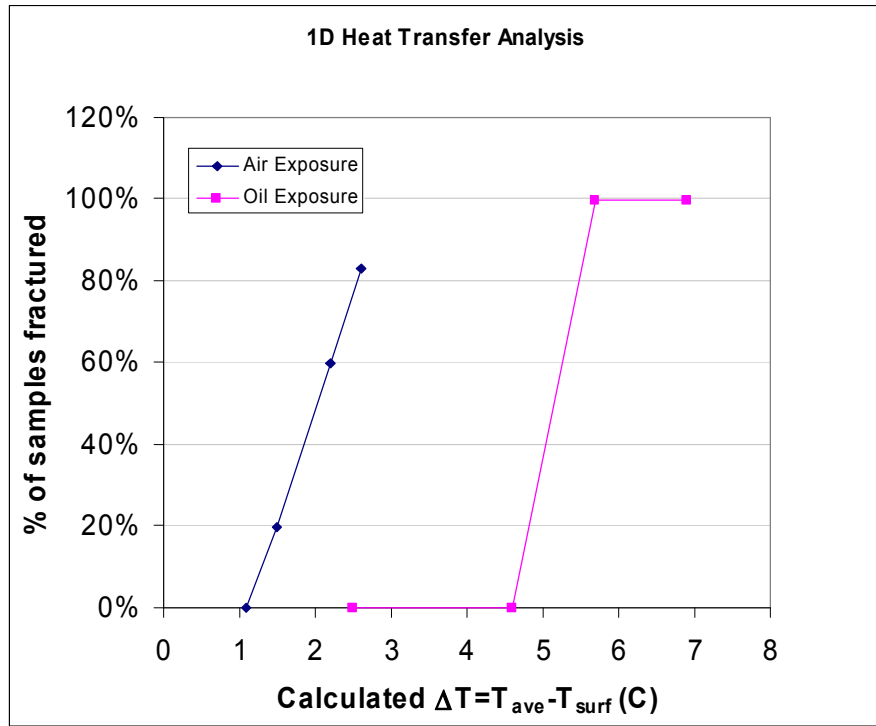
theory of solids[3]. Note that stress and strain are tensor quantities. This analysis shall be performed at a later date time permitting. Another explanation for the discrepancy is that moisture enhanced sub-critical crack growth can occur in samples exposed to air. Therefore, a flaw on the crystal can grow to critical flaw size and then fracture even though initially the sample had a stress that was below the critical stress for failure.

Despite the discrepancy in ΔT between oil and air exposed samples, the air exposed samples were observed to fracture with $\Delta T = T_{\text{ave}} - T_{\text{surf}}$ of greater than 1°C . Fracture probability becomes 100% for a $\Delta T > 2.5^\circ\text{C}$. We will use this criteria ($\Delta T < 1^\circ\text{C}$) for fracture of DKDP crystals exposed to an air environment.

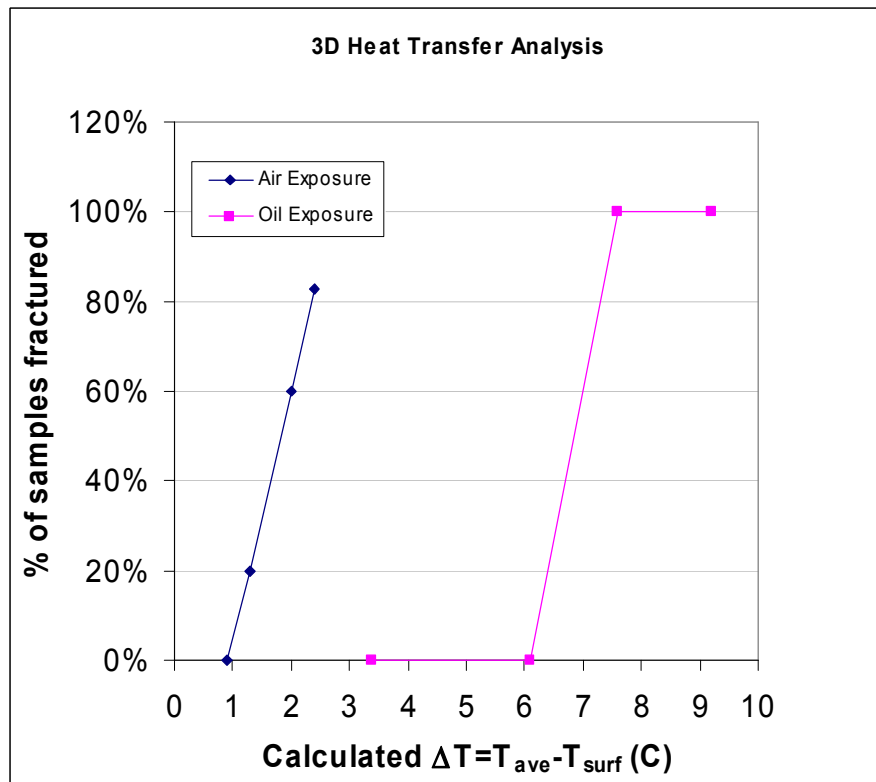
A few additional thermal shock experiments were conducted to examine the fractography of the fractures. Three conditions were examined. The first sample originally at 80°C was placed on fiber insulation in air (Fig. 8a) (same as reported in Table 4). The fracture originated from the top edge near the center of the sample and propagated initially perpendicular to the top surface and vertical surface and vertical surface. This indicates that the combination of peak tensile stress and largest flaw are present on the 2D edge of the material. We would expect the ΔT to be higher on the top surface because that is where the heat loss is taking place; little heat loss is taking place at the fiber insulation. Surprisingly, fracture did not take place at the corner where ΔT is the largest.

The second sample is similar to the first except that hot H_2O was placed on the top surface. A series of spider cracks on the top surface were observed (Fig. 8b). In this case the rapid heat loss due to evaporation lead to large temperature difference (hence large tensile stress) over a thin layer on the surface. Notice that the fractures did not originate from the 2D edge.

The third sample was placed on an aluminum plate at room temperature. This sample fractured immediately originating from the bottom 2D edge of the sample. This indicates that the combination of peak tensile stress and largest flaw are present on the 2D edge of the material. Again, the fracture propagated perpendicular to the top surface first. The heat transfer coefficient for Al is about 2000 times faster than air.



(a)



(b)

Figure 8. (A) % of DKDP samples fractured used in the thermal shock experiments vs that calculated $\Delta T = T_{ave} - T_{surf}$ in the sample using 1D heat transfer analysis. (b) same as (a) except ΔT was calculated using the 3D heat transfer analysis. Note T_{surf} for the 3D case is the temperature at the surface at the center top edge of the sample where the fracture originated.

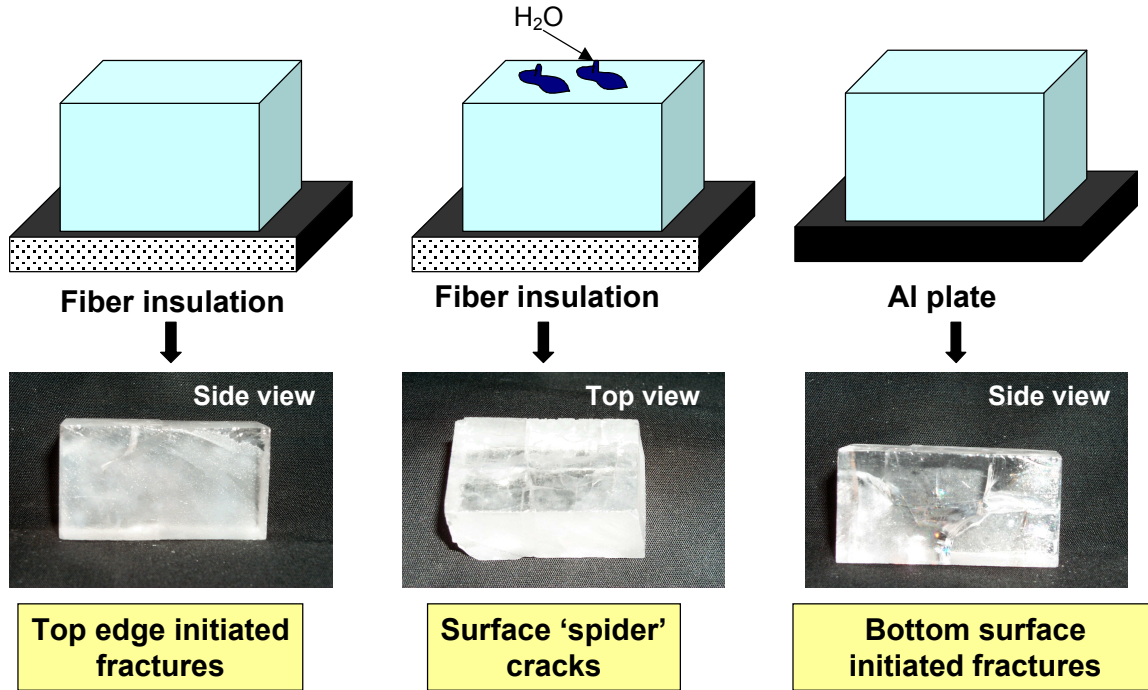


Figure 9: Comparisons of the types and location of fractures observed depending on method of quenching. The quench type determined the location in the sample where the temperature difference and hence the magnitude of the stress is highest.

B. Verification of h for air

Because of the large discrepancy ΔT measured for oil and air to cause failure, we decided to check the value of h for air since it is largely dependent on the velocity of air passing by the sample. In this experiment, a thermocouple was placed near the center/bottom surface of the DKDP crystal previously heated to 74.4 °C in the oven. The sample was placed on fiber insulation, same as in the thermal shock experiments discussed above. The temperature was then monitored on the bottom surface. Using the 3D heat analysis, the best value of h was chosen. A heat transfer coefficient of $h = 10 \text{ W/m}^2\text{K}$ is a good value for air (see Fig. 10). Note the deviation of the measured data from the calculation at short times is due to heat taken away by the thermocouple itself. Also the deviation in the long time is due to not taking account radiation in this particular simulation.

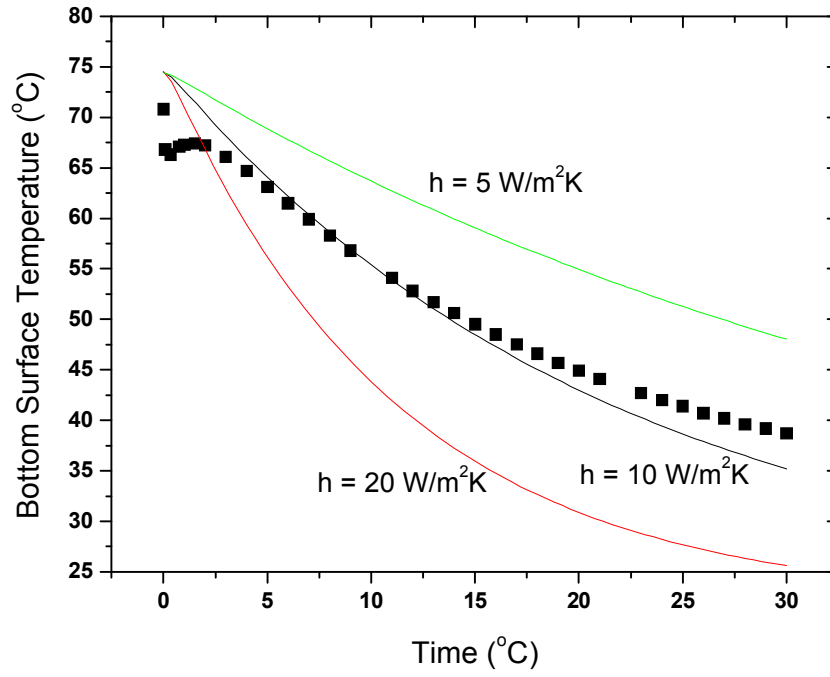


Figure 10. Temperature on the bottom center of $2.5 \times 2.5 \times 5.0 \text{ cm}^3$ DKDP place on fiber insulation as a function of time. The crystal at time zero was initially at $74.4 \text{ }^\circ\text{C}$. The points represent the collected data and the lines represent calculated values using the 3D heat transfer analysis using different heat transfer coefficients.

V. EXPLANATION OF LARGE SIZE FRACTURES & RECOMMENDATIONS FOR FRACTURE MITIGATION

We now examine three cases of previously observed fractures of large DKDP boules and compare them to the calculations of ΔT to see if they make sense. This should provide confidence that the calculations are reliable. The third case is examined in the most detail because it is the most relevant case in the cooling of a large DKDP boule from 50°C to room temperature.

Case 1: Crystal F-8. This crystal was grown to a size of ~250 kg. The growth stopped at 26°C, and the salt solution was removed from the growth tank. Afterward, the heater to water bath was turned off, but the chiller was left on. Hence the temperature of the water, dropped to 9.7°C after ~5 hours. Correspondingly, the growth tank temperature dropped to 12°C. The crystal was observed to fracture catastrophically, initiating in several places. The fractures are shown schematically in Fig. 10.

Assuming the crystal surface was originally at 26°C and drops to 12°C in 5 hours, and assuming the crystal is a cube (47 x 47 x 47 cm³), the 1D ΔT =4.8°C (at 5 hours) is and the 3D ΔT is 4.4°C (Fig.11). This ΔT is more than high enough to cause failure based on our criteria of 1°C.

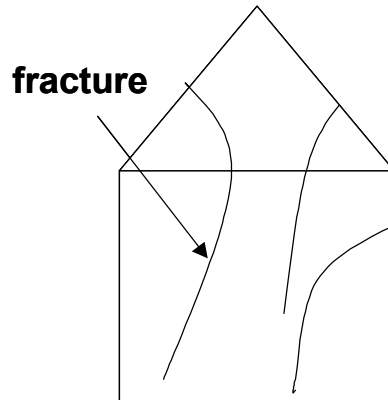


Figure 10. Schematic of the fracture of F-8 crystal (Case 1).

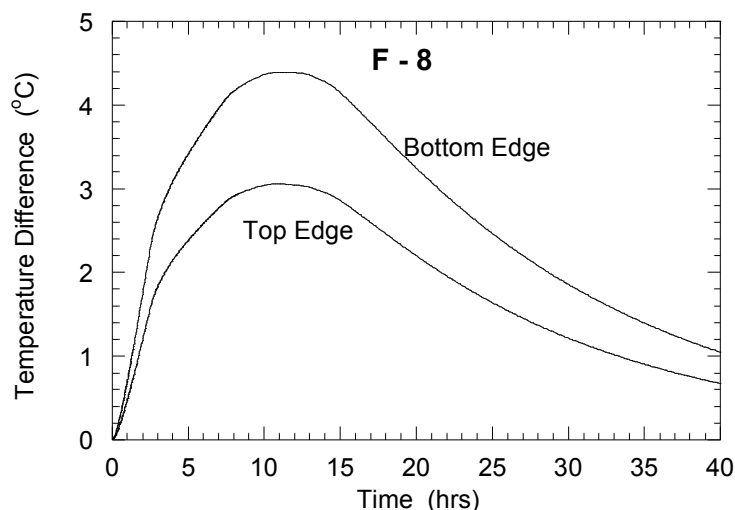


Figure 11. Calculated $\Delta T = T_{ave} - T_{surf}$ for cooling of crystal F-8.

Case 2 Crystal E-2. This crystal was grown to a size of \sim kg. The growth stopped at 20°C, and the salt solution was removed from the growth tank. The crystal was removed from the tank and placed in the room near an air conditioning vent. We guess that the temperature of the air hitting the crystal was 16°C. Judging by the fracture drawing, which are described in more detail elsewhere [7], the fracture clearly originated from the bottom 2D edge of the crystal which was in contact with the Al platform. Comments in the memo[7] refer to an air conditioner vent near the crystal and Al platform. The cool air must have cooled the Al platform, which in turn took away heat from the bottom of the crystal. Evaporation of solution may have also played a role when the crystal was separated from the Al platform.

We assume the crystal surface was originally at 20°C and drops to 16°C instantaneously where the Al platform is located. Using a heat transfer coefficient of 20,000 W/m²K, the calculated 1D $\Delta T = 3.5^\circ\text{C}$ and the 3D $\Delta T = 2.7^\circ\text{C}$. Again, this ΔT is large enough to cause fracture.

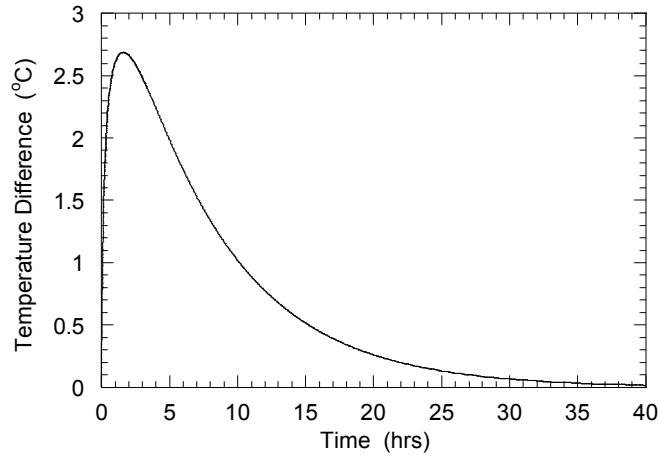


Figure 12. Calculated $\Delta T = T_{\text{ave}} - T_{\text{surf}}$ for cooling of crystal E-2.

Case 3: FD-16. This crystal was a horizontal growth crystal that grew to a size of $30.5 \times 19 \times 7.5 \text{ cm}^3$. At the end of growth, the final salt solution temperature was 62°C and the solution was removed at 1 liter/min. Hot dry air was input at a rate of approximately 80 slm from the CFS into the growth tank during the solution removal. The temperature of the air in the grow tank did not change much from the solution (60°C). The bath was then cooled at $3^\circ\text{C}/\text{day}$ to room temperature (25°C). A single fracture was observed propagating through the center of the crystal (see Fig. 13).

A more detailed analysis of the fracture surface is shown in Fig. 14. Using common fractography analysis, the origin point of the fracture was evaluated[8]. It is clear that the fracture originated from the bottom side of the pyramid face. The exact origin point is not as conclusive. Most of the fracture marks near the origin point are removed because salt solution penetrated into the crack and dissolved the surface. However, based on the presence of some subtle Walner lines near the origin, the fracture is believed to be originated from the pyramid corner (See Fig 14b.)

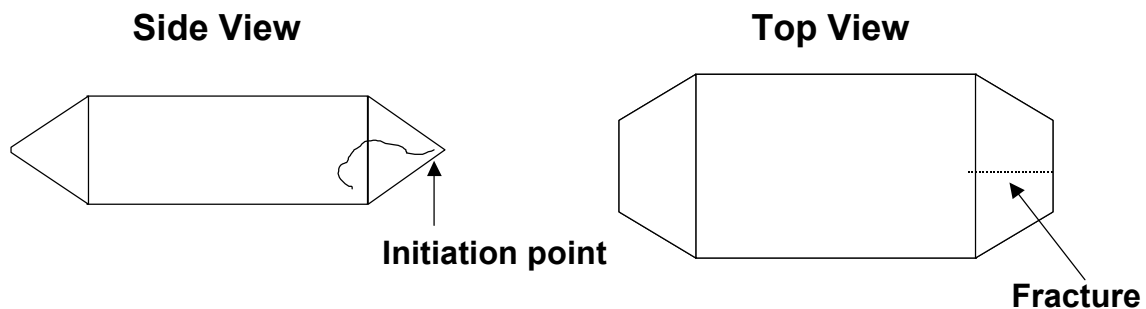
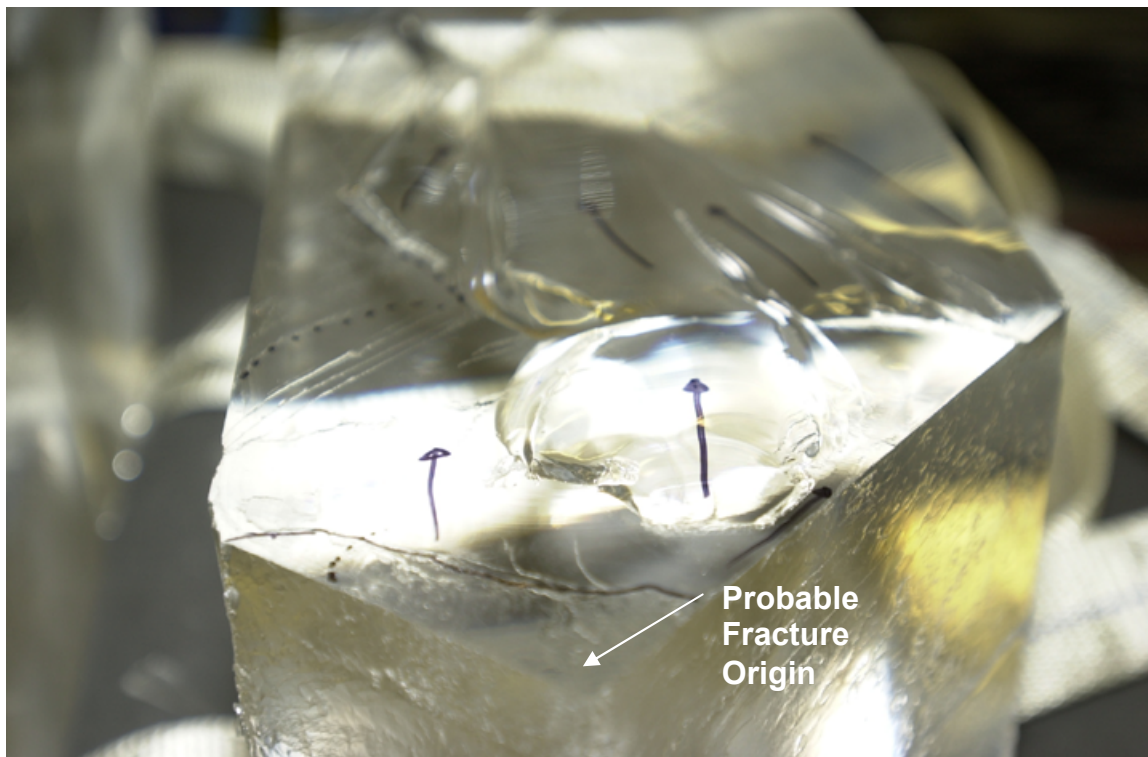


Figure 13. Schematic of observed fracture of FD16.



(a)



(b)

Figure 14. Fracture surface of FD-16. Black arrow indicate direction of fracture. Dashed lines are traces of some observed Wallner lines. Black line indicates region where salt solution penetrated into fracture and dissolved surface.

There are a number of possible causes for this fracture, which are summarized in Table 6. In each of these cases, the ΔT was calculated (see Fig. 15) in order to determine if it enough to lead to failure. Only the 3D ΔT is reported in the table. It is clear that cooling the crystal at 3°C/day and a temperature drop in a seal volume should not cause fracture. However, evaporation off the crystal and heat escape from the metal platform could lead to fracture. Based on the fractography analysis, the crystal did not appear to initiate at the contact point with the aluminum platform. Hence, the major contributor to stress is likely the evaporation off of the crystal.

Table 6: Possible scenarios that could cause fracture in FD-16.

Possible Cause	Simulation conditions	Calculated ΔT	Conclusion
1) Nominal cooling rate was too fast	Cool crystal in air	0.18 °C	Should not Fracture
2) Air temperature drop upon solution removal	Cool crystal in air in sealed tank; initial air input is at 25oC	0.92 °C	Fracture not likely
3) Evaporation off crystal surface	Cool crystal in air in sealed tank; heat loss from evaporation on all sides of crystal	5.7 °C	Fracture!
4) Heat escape from metal platform (conduction loss)	No evaporation; conduction loss from platform	2.2 °C	Fracture!

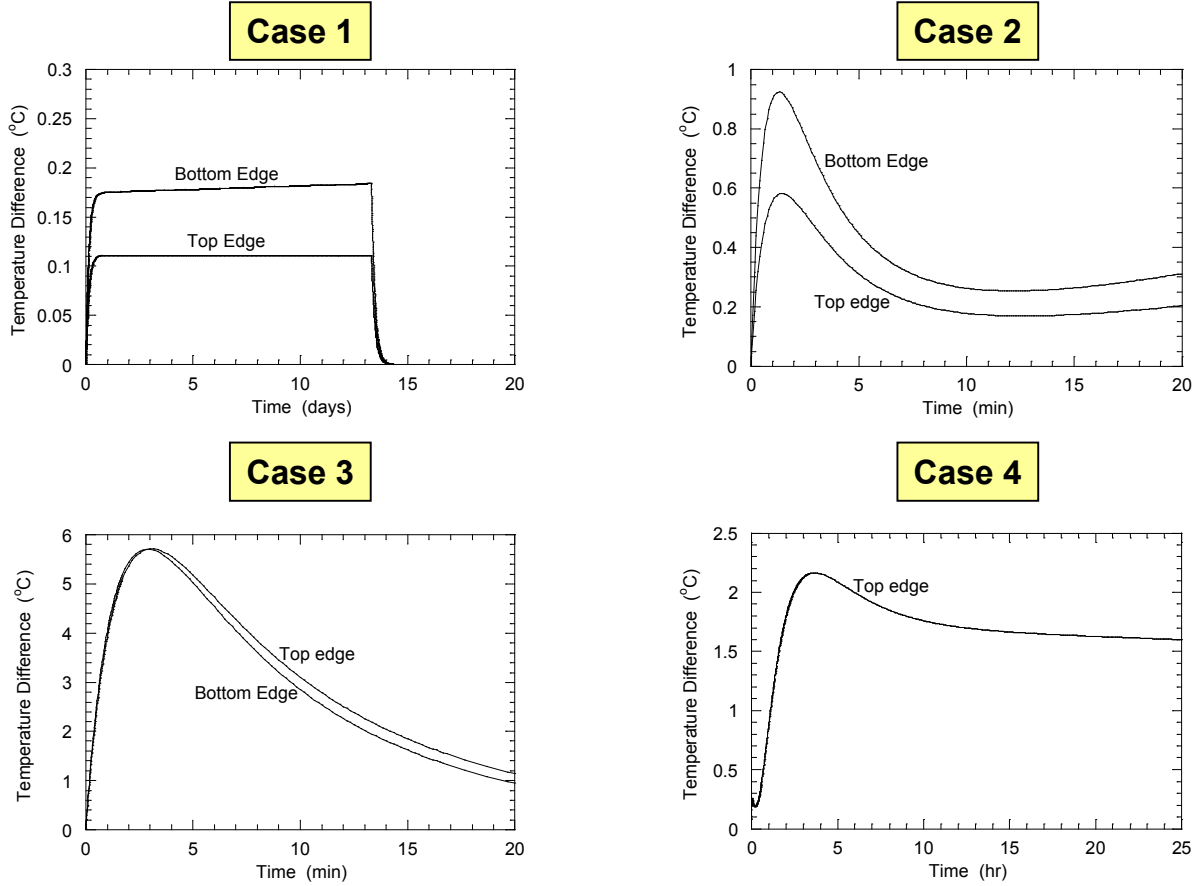


Figure 15. Calculated $\Delta T = T_{\text{ave}} - T_{\text{surf}}$ for cooling of crystal E-2 using different cases described in Table 6.

Proposed Mitigation Strategy.

The proposed mitigation strategy is to input temp matched saturated air into the growth tank as the salt solution is being removed from the growth tank. This should eliminate any heat loss due to evaporation. After the salt solution is removed, the saturated air input can be stopped and the crystal should be cooled at 3°C/day to room temperature. Fig. 13 schematically shows one method where saturated air can be input into the growth tank.

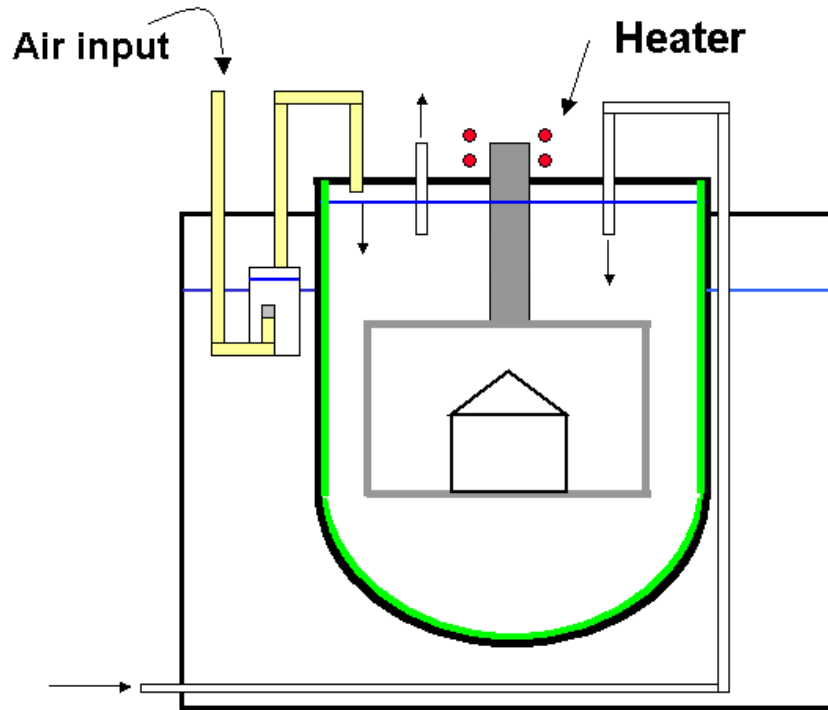


Figure 13: Schematic of growth tank at end of run. Solution is at 50°C and salt solution is removed at 1 liter/min and saturated air to be input at 1 liter/min.

Conclusions

Heat transfer analysis, thermal shock experiments, and fractography have been used to evaluate the tendency for DKDP to fracture under thermal stress. Based on this, DKDP with a rough finish (flaw size, approximately several hundred microns) has the possibility for fracture if it has a $\Delta T = T_{\text{ave}} - T_{\text{surf}} > 1^\circ\text{C}$. This criteria matches coincides with previous large crystal that have fractured. Evaluation of a crystal (FD-16) that fractured at the end of a ‘high’ temperature run, reveals that solution evaporation off the crystal surface likely contributed to the fracture. Hence a mitigation strategy is proposed to input bath temperature matched-saturated air upon solution removal at the end of ‘high’ temperature growth run.

References

1. T. Anderson, "Fracture Mechanics: Fundamentals and Applications", 2nd Ed, CRC Press, Boca Raton (1995)
2. T. Suratwala, T. Land, W. Seikaus, T. Huser, C. Hollar, R. Floyd, A. Burnham, R. Steele, "D/H Diffusion in DKDP: Part 1: Diffusion and Stress Development", NIF 0071473, Dec. 15, 2001
3. S. Crandall, "An introduction to the mechanics of solids", McGraw-Hill, New York (1959)
4. W. Kingery, H. Bowen, D. Uhlmann, "Introduction to Ceramics", John Wiley & Sons, New York, Chapter 16 (1976)
5. J. VanSant, "Conduction Heat Transfer Solutions", LLNL, UCRL-52863 Rev. 1, page 8-5 (August 1983).
6. Cleveland Crystals Inc. Product Information Sheet, Box 17151, Cleveland Ohio.
7. R. Hawley-Fedder, "Cracking of KDP boule E-2 during removal from the platform", LLNL internal memo, December 10, 1998.
8. J. Varner, V. Frechette, "Fractography of Glasses and Ceramics", Advances in Ceramics, Vol. 22 (1988)